A modern ionotropic glutamate receptor with a K$^+$ selectivity signature sequence

H. Janovjak[$,1,2], G. Sandoz[$,1,3] and E.Y. Isacoff[1,4,]*

[1] Department of Molecular and Cell Biology and the Helen Wills Neuroscience Institute, 271 Life Sciences Addition, University of California, Berkeley, CA 94720, USA

[2] Current address: Institute of Science and Technology Austria, Am Campus 1 A-3400 Klosterneuburg, Austria

[3] Institut de Pharmacologie Moléculaire et Cellulaire, CNRS, and Université de Nice Sophia-Antipolis, Sophia-Antipolis, 06560 Valbonne, France

[4] Physical Bioscience Division and Material Science Division, Lawrence Berkeley National Laboratory, Berkeley, CA 94720, USA

$ These authors contributed equally to this work.

* Correspondence should be addressed to E.Y.I. (ehud@berkeley.edu).

Abstract

Glutamate is the major excitatory neurotransmitter in the mammalian central nervous system and gates non-selective cation channels. The origins of glutamate receptors are currently not understood as they differ structurally and functionally from simple bacterial ligand-gated ion channels. Here, we report the discovery of an ionotropic glutamate receptor that combines the typical eukaryotic domain architecture with the 'TXVGYG' signature sequence of the selectivity filter found in K^+ channels. This receptor exhibits functional properties intermediate between bacterial and eukaryotic glutamate-gated ion channels, suggesting a link in the evolution of ionotropic glutamate receptors.

Main text

Rapid signal transduction in the central nervous system of vertebrates relies on the neurotransmitter glutamate (Glu) and ionotropic glutamate receptors (iGluRs)[1]. Historically, iGluRs were grouped according to their responses to the small molecule agonists AMPA (α-amino-3-hydroxyl-5-methyl-4-isoxazolepropionic acid; GluA1-A4), kainate (GluK1-K5) and NMDA (*N*-methyl-D-aspartate; GluN1, GluN2A-D and GluN3A and B). The origins of iGluRs form the basis of their functional and structural diversity but are currently not understood[2-4]. Simple bacterial iGluRs, such as GluR0 from *Synechocystis*, presumably arose from the fusion of periplasmic binding proteins (PPBP) and K$^+$ channels (**Fig. 1a**, left)[4-7]. GluR0 differs in several major ways from its metazoan and plant homologues[5]. Structurally, it has only two transmembrane (TM) segments, instead of three, and no N-terminal domain (NTD) (**Fig. 1a**). Functionally, it distinguishes itself from the non-selective cation permeation of iGluRs in being K$^+$-selective because of its pore loop (P-loop), which contains the 'TXVGYG' signature sequence of the K$^+$ channel selectivity filter (**Fig. 1b**). Pharmacologically, GluR0 is activated by amino acids other than Glu, but not by classical iGluR agonists.

The complex domain architecture shared by eukaryotic iGluRs (**Fig. 1a**, middle) suggests a common eukaryotic ancestor[2, 8] that may merge elements of GluR0, like the K$^+$ selectivity filter, with those of iGluRs, like the NTD or C-terminus. In this study, we report the discovery and functional characterization of AvGluR1, which is the first eukaryotic iGluR with the complex architecture of vertebrate iGluRs and the signature sequence of the K$^+$ channel selectivity filter. Domain organization and function seem to indicate that AvGluR1 represents the "transitional stage" between bacterial and vertebrate iGluRs.

Results

Identification and structure

We searched the eukaryotic protein database of the National Center for Biotechnology Information (NCBI) with artificial sequences that combined a mammalian LBD and C-terminus (either from GluK2, GluA2 or GluN1) with a K$^+$ selectivity filter (from GluR0, **Methods**). The only protein returned by these searches that aligned to iGluRs over all domains was a putative iGluR from the fresh-water bdelloid rotifer *Adineta vaga*, a remarkable model organism for asexual reproduction and horizontal gene transfer (HGT) whose genome has been partially sequenced[9]. We termed this uncharacterized iGluR AvGluR1. The domain organization of AvGluR1 mirrors that of eukaryotic iGluRs (**Fig. 1a**, right). It features the 'SYTAXLA'-motif in TM2 that is conserved in all known eukaryotic iGluRs[3] (**Fig. 1b**) but contains a 'TXVGYG'-motif in its P-loop, as in GluR0 and K$^+$ channels. Consequently the P-loop of AvGluR1 aligns most closely to that of K$^+$ channels, while the remainder of the TM domain resembles that of iGluRs (**Supplementary Table S1**). The

LBD exhibits weaker similarity to both eukaryotic iGluRs and GluR0, but an arginine residue that contacts the ligand's α-carboxyl group in all mammalian iGluRs (e.g. R523 in GluK2) is conserved in AvGluR1 (R546) and so is an acidic residue contacting the α-amino group (E738 in GluK2), which is an aspartic acid in AvGluR1 (D744) and in all NMDA receptors (**Supplementary Fig. S1**). Residues contacting the γ-carboxyl of Glu are not conserved in AvGluR1 (e.g. T690 in GluK2 is A704 in AvGluR1, like in GluN3A and B but in no other iGluR) and AvGluR1 can gate upon binding amino acid ligands other than Glu (see below). There is low conservation of the NTD of GluK2 compared to AvGluR1 (**Supplementary Table S1**) and to other lower invertebrates (data not shown), except for two marked cysteine residues (**Supplementary Fig. S1**) that stabilize the NTD in all mammalian iGluRs[10]. Finally, AvGluR1 has a C-terminus that is 43 amino acids in length whose sequence shows no homology to any known protein. Similarly, no homologues are found for the C-termini of many iGluRs of lower invertebrates (data not shown).

Functional characterization

When we expressed AvGluR1 in *Xenopus leavis* oocytes we recorded large currents in response to Glu perfusion (**Fig. 2a** and **3a**). Like GluR0, AvGluR1 was gated by Glu with high potency (EC50 = 4.0 μM; 95 % confidence interval 0.8 to 20.0 μM, N = 7; **Fig. 2b**). AvGluR1 was also gated by several other amino acids, including aspartate, serine, glutamine, and, very weakly, by glycine (**Fig. 2a**). Glycine had no effect on the response to Glu (**Supplementary Fig. S2**). These amino acids do not gate AMPA and kainate receptors but serve as agonists of NMDA receptors[5, 11-13]. AvGluR1 was also gated by iGluR agonists kainate and AMPA (**Fig. 2a** and **Supplementary Fig. S3**), as observed for mammalian receptors, but not for GluR0[5, 11, 12, 14]. For aspartate and kainate, the difference in agonist response seems to be due to a shift in potency since the currents extracted from the fit at the EC50 concentration are in the same range as for Glu (**Supplementary Fig. S3**).

AvGluR1 currents activated slowly but exhibited full desensitization to prolonged agonist application (**Fig. 2a, 2c** and **3a**). The slow activation of AvGluR1 resembles the behavior of GluR0, and is distinct from the rapidly activating iGluRs (**Fig. 2c**), whereas the full desensitization resembles the behavior of iGluRs, but differs from GluR0, which only desensitizes partially[5]. Slow activation was also observed when agonist was presented by photolysis of caged-L-glutamate (**Fig. 2d** and **e**).

Finally, despite having a K^+ channel type selectivity filter sequence, AvGluR1 exhibited a poor selectivity for K^+ over Na^+, similar to that of vertebrate iGluRs. Analysis with the Goldman-Hodgkin-Katz equation indicates a P_{Na+}/P_{K+} permeability ratio of 0.3 (*versus* 0.01 for GluR0 and0.8 for GluK2[5, 15]) (**Fig. 3a** and **Supplementary Fig. S4**). To test for Ca^{2+} permeability, we

compared currents recorded in normal extracellular solution (containing 1.8 mM Ca^{2+}) and in the absence of Ca^{2+} (zero added extracellular Ca^{2+} with 0.5 mM EGTA). Neither current amplitude nor reversal potential differed between these conditions (**Fig. 3a** and **b**). Moreover, the Ca^{2+}-activated Cl^--channels of Xenopus oocytes[16] did not contribute to the current, since replacing external Cl^- did not modify either Glu-evoked current amplitude or reversal potential of AvGluR1. These data indicate that the channel has little or no permeability to Ca^{2+} (**Fig. 3a** and **b**).

Together, amino acid sequence, domain organization, and function indicate that AvGluR1 represents a functional intermediate between GluR0 and iGluRs.

Phylogenetic analysis

To further examine the relationship between AvGluR1 and iGluRs, we performed a phylogenetic analysis of 251 iGluRs sampled from bacteria, plants and animals (**Supplementary Table S2** and **S3**). In particular, we collected all iGluR-like proteins from the few early branching animals that have such sequences (e.g. *Trichoplax adhaerens*, the cnidarian *Nematostella vectensis* or the mollusk *Aplysia californica*). Phylogeny was inferred using several methods including maximum likelihood (ML) with RAxML[17]. In the ML phylogeny (**Fig. 4**), AvGluR1 branches out early compared to all other metazoan iGluRs with bootstrap support of 77 and 85 %. Trees built using different ML methods and neighbor joining yielded the same branching order and similar bootstrap support, as did trees build on a larger dataset automatically collected by FlowerPower[18], and if the GYG-sequence in AvGluR1 was replaced by three consecutive glutamines to mimic non-NMDA iGluRs (data not shown). This branching order supports the functional analysis and suggests that AvGluR1 represents a transitional stage between bacterial and metazoan iGluRs. In particular, the phylogenetic analysis allows excluding the possibility that AvGluR1 arose from the secondary acquisition of the 'TXVGYG'-sequence by a rotifer iGluR. In such a re-evolution scenario, the overall sequence of AvGluR1 should resemble that of iGluRs from animals that started to develop independently before and after rotifers. Phylogenetic analysis would then place AvGluR1 deep within the animal part of the tree, which is not observed.

Discussion

The origins of iGluRs are mysterious[2-4]. Our own database search (**Methods**) confirmed that iGluRs are absent from basal eukaryotes, such as fungi, protozoa or the sponge *Amphimedon queenslandica*[2, 19]. We cloned and characterized an iGluR whose amino acid sequence, domain organization and function resembles the missing intermediate between bacterial and eukaryotic iGluRs. In the *A. vaga* genome, the gene coding for AvGluR1 is located near transposable elements[9] and we cannot exclude that it originates from HGT[20]. The existence of bacterial ion

channels with an LBD but without K$^+$ selectivity motif raised the question which class of proteins developed into iGluRs[21]. Our findings suggest that iGluRs evolved by addition of an NTD and TM3 to a GluR0-like protein that contained a 'TXVGYG'-motif. These new domains endow new functionalities to iGluRs, in that NTDs provide for sub-type specific assembly and modulation of gating, while the third TM helix locates the C-terminus intracellularly for sorting, binding to the cytoskeleton and modulation[1]. The promiscuous agonist binding of AvGluR1 is divergent from typical AMPA, kainate or NMDA receptors and rather resembles that of chemosensory receptors in single cell organisms and sensory cells of multicellular organisms[22]. Indeed, iGluR-like chemosensors that lack an NTD were recently identified in the fruit fly, and it will be interesting to see how these proteins and AvGluR1 accommodate a chemically diverse spectrum of ligands. The low conservation of the NTD and C-terminus of AvGluR1 may not be surprising as this receptor likely serves different roles than modern neurotransmitter receptors for which cytosolic association and modulation are crucial. The identification of AvGluR1 and voltage-sensing phosphatases[23] thus re-emphasizes that exotic invertebrates offer a repertoire of novel proteins that remain to be discovered.

Methods

Uniprot accession numbers

The following sequences were used for the alignment of **Fig. 1** and **Supplementary Fig. S1** (Uniprot identifiers in parentheses): *R. norvegicus* GluK2 (P42260), *A. thaliana* Glr2.1 (O04660), *Synechocystis* GluR0 (P73797), *S. lividans* KcsA (P0A334), *A. pernix* K$_v$ (Q9YDF8) and *D. melanogaster* Shaker (P08510). Sequences were aligned using Muscle 3.8[24] with the default parameters.

AvGluR1 identification and bioinformatics

AvGluR1 (Uniprot identifier B3G447) was identified in the NCBI non-redundant protein database using a search with PHI-Blast. The primary query sequence was a chimeric protein of GluK2 (from *R. norvegicus*, LBD, TM3 and C-terminus, residues 426 to 556 and 658 to 908) and GluR0 (from *Synechocystis* PCC 6803, pore domain, residues 154 to 246). Residues are numbered beginning with the start-methionine. The query was limited to eukaryotes (taxonomy ID 2759) and the PHI-pattern [TVIL]-G-[YF]-G-[DFLYGHKARN] that covers the K$^+$ selectivity filter of a majority of K$^+$ channels[25]. As of August 25 2010, AvGluR1 is the highest ranking hit for this query (27% identity) and the only hit aligning over close to the entire length of the protein. Identical queries using the LBD, TM3 and C-terminus taken from the GluA2 AMPA receptor (from *R. norvegicus*, Uniprot identifier Q9R174, residues 409 to 539 and 644 to 883) or the GluN1 NMDA receptor

(from *R. norvegicus*, Uniprot identifier P35439, residues 413 to 555 and 654 to 938) also yielded AvGluR1 as the highest ranking hit.

Preparation of expression constructs

The a-splice isoform of GluK2 was obtained from K. Partin (Colorado State University, Fort Collins, Co) and cloned into pGEM-HE. Genomic DNA of *A. vaga* was a kind gift of E. Gladyshev and I. Arkhipova (Marine Biology Laboratory, Woods Hole, MA and Harvard University, Cambridge, MA). Forward (TAT CCC GGG CAC CAT GAG AAT ATT TCG AGA AAA CAT CTC GTG) and reverse (ATA TCT AGA TTA TGC AAT GAT TTG TGA TAT AGT AGA CGA AG) oligonucleotide primers for polymerase chain reaction (PCR) included XmaI and XbaI restriction sites for subcloning into pGEM-HE. PCR reaction parameters were: One cycle (95 °C for 60 s); 32 cycles (95 °C for 30 s, 56 °C for 30 s, 72 °C for 180 s), one cycle (95 °C for 10 min). Several independent PCR reactions yielded the same AvGluR1 sequence that differs from that deposited in genome sequencing in 26 positions (**Accession Codes**).

RNA preparation and electrophysiology

RNA was transcribed by using mMessage mMachine T7 transcription kit. Surgically extracted *X. laevis* oocytes were injected with 5 ng of RNA in 50 nL volume. Cells were incubated in ND-96 solution (96 mM NaCl, 2 mM KCl, 1.8 mM $CaCl_2$, 1 mM $MgCl_2$, 50 mgmL^{-1} gentamicin, 2.5 mM sodium pyruvate, and 5 mM Hepes, pH 7.4) at 18 °C for 12–36 h before experiments. Cells expressing GluK2 were pre-treated with concanavalin-A. Two-electrode voltage-clamp (TEVC) was performed at room temperature with a Dagan CA-1B amplifier, Digidata-1440A data acquisition board and pClamp10 software. Oocytes were placed in a perfusion dish and recordings were performed in ND-96 recording solution without antibiotics. For uncaging the MNI-caged-glutamate, illumination was done with a 150 W xenon lamp through a Nikon Diaphot inverted microscope with a 20× 0.75 NA fluorescence objective (Nikon). Illumination time was defined by a Uniblitz shutter (Vincent Associates) controlled by the Digidata-1440 board and pClamp10 software package (Axon Instruments).

Data analysis

To estimate relative permeabilities of Na$^+$ and K$^+$ we analyzed reversal potentials using the simplified Goldman-Hodgkin-Katz voltage equation, $P_{Na+}/P_{K+} = \exp(\Delta E_{rev}F/RT)$, where ΔE_{rev} is the reversal potential difference between Na$^+$ and K$^+$, F Faraday's constant, R the gas constant and T temperature and after correction for liquid junction potentials. To determine the EC50 (**Fig. 2** and **Supplementary Fig. S3**), dose–response data were fit in SigmaPlot with the Hill equation $I=x^h/(x^h+EC50^h)$, where I represents the normalized current, x represents concentration, and h is the Hill Coefficient.

iGluRs in archaea and unicellular eukaryotes

To identify iGluRs in archaea and unicellular eukaryotes, we searched the non-redundant protein database of the NCBI with Blast. We used GluK2 from *R. norvegicus* as the query sequence and limited the search to archaea (2157), funghi (4751), monosiga (81525), diatoms (2836), alveolata (33630), trypanosome (5690) and dictyostelium (5782; numbers in parentheses are taxonomy identifiers). As of August 25 2010, highest-ranking hits were K^+ channels or completely unrelated proteins with E-values near zero. No proteins that contain an iGluR-like LBD and TM domain could be identified.

Phylogenetic analysis

Using Blast searches, we identified 251 iGluR-like proteins in bacteria, plants and animals with special attention to early branching eukaryotes (**Supplementary Table S2**). For these organisms, we collected all proteins that aligned to AvGluR1 or GluK2 over the pore and LBD. This dataset included iGluRs that were identified previously, as well as sequences that have not yet been annotated (**Supplementary Table S3**). This search also revealed AvGluR2 (Uniprot identifier B3G464), an *A. vaga* protein that features the TXVGYG-pore motif and shares 53% sequence identity with AvGluR1. Sequences were aligned with Muscle[26]. Gaps and the N- and C-terminal domains only found in eukaryotic proteins were manually removed. Phylogenetic analysis was primarily performed with the maximum likelihood (ML) method and RAxML 7.2.6[17]. 20 ML searches were conducted to find the best ML tree (**Fig. 4**) and branch support was assessed with 100 bootstrap replicates. We observed the same branching order of AvGluR1 in trees that were built with different amino acids substitution matrices, through neighbor joining with BioNJ[27] and based on a dataset of 606 proteins automatically collected with FlowerPower[28] followed by neighbor joining.

Author Contributions

H.J. and G.S. designed and performed experiments, analyzed data and wrote the paper; E.Y.I. designed experiments, analyzed data and wrote the paper.

Competing Financial Interests

The authors declare no competing financial interests.

Supplementary Information

Supplementary Figures S1-4 and Supplementary Tables S1-3

Accession Codes

Sequences of AvGluR1 and AvGluR2 have been deposited in GenBank under accession codes HQ901600 and HQ901601.

Figures
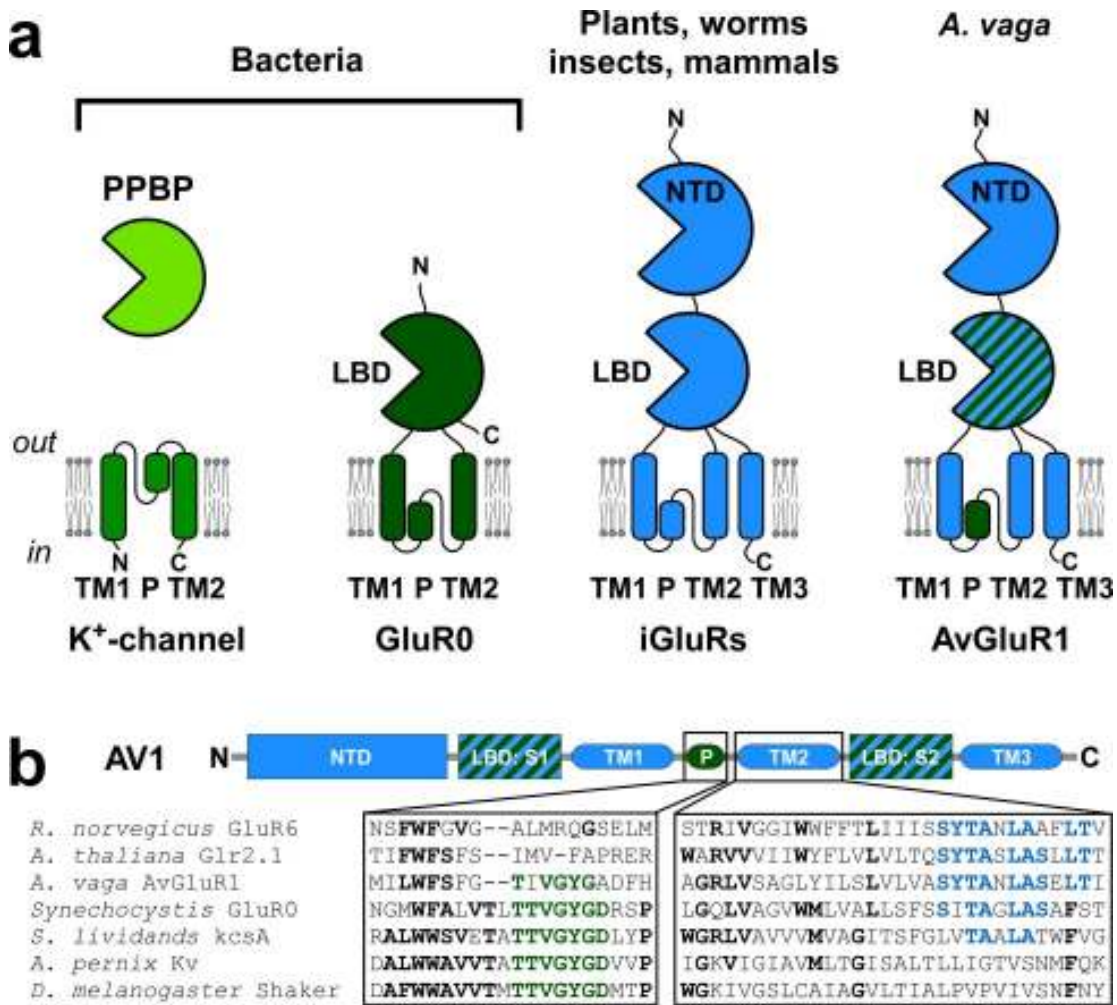
Figure 1. Origins of iGluRs. (**a**) TM and domain organization of iGluRs, AvGluR1 and proteins resembling bacterial ancestors. Color shading is based on sequence identities of individual domains (also see **Supplementary Table S1**). (**b**) Sequence alignment of P-loop and TM2 for AvGluR1, iGluRs from mammals and plants, GluR0 and K$^+$ channels. Residues found in at least three sequences are highlighted in bold. Colors highlight conserved motifs.
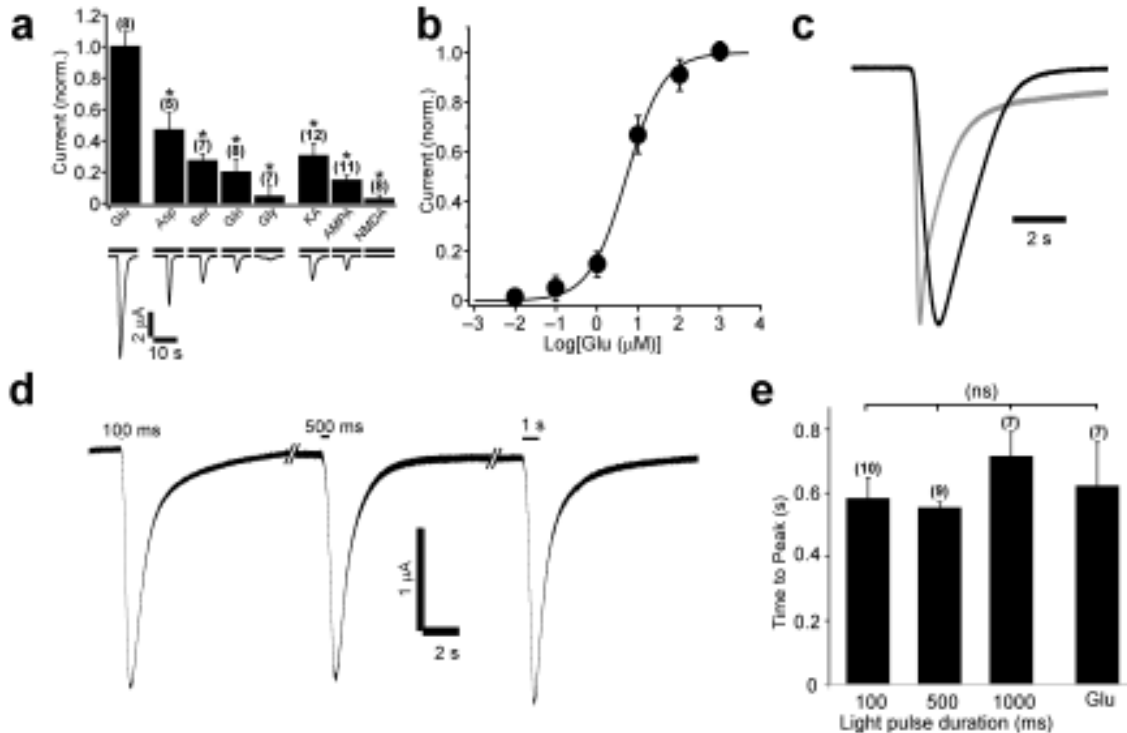
Figure 2. Agonist specificity and slow gating of AvGluR1. (**a**) Agonist specificity measured for 1 mM agonist concentration. Traces of single cell responses to various agonists (bottom). Bar graphs show average current amplitudes $\pm$ s.e.m. for multiple cells (top). *F-test analysis of variance showed that agonist responses are significantly different at the 1% level (P < 10^{-10}). Post-hoc analysis using the Tukey-Kramer method showed that the response to Glu is different from that of all other agonists at the 1% significance level (P < 0.0001 for each pair-wise comparison). (**b**) Peak AvGluR1 response to 15 s application of Glu at various concentrations (mean $\pm$ s.e.m. from 7 oocytes). Data were fit as described in the Methods (EC50 = 4.0 μM, 95 % confidence interval 0.8 to 20.0 μM, h = 1.0, n = 7). In (a) and (b) agonists were applied at 3 min intervals to allow recovery from desensitization. (**c**) Normalized currents of GluK2 (grey trace) and AvGluR1 (black trace) elicited by prolonged 1 mM Glu application reveal slow activation of AvGluR1. (**d**) Currents elicited by 20 µM MNI-caged-L-glutamate released by light pulses of different duration also rise slowly. (**e**) Time to peak of AvGluR1 currents elicited by Glu uncaging or perfusion (ns indicates no statistically significant differences using the Student's *t*-test, P $\geq$ 0.2). In (**a**) and (**e**) number of observations shown in parentheses.
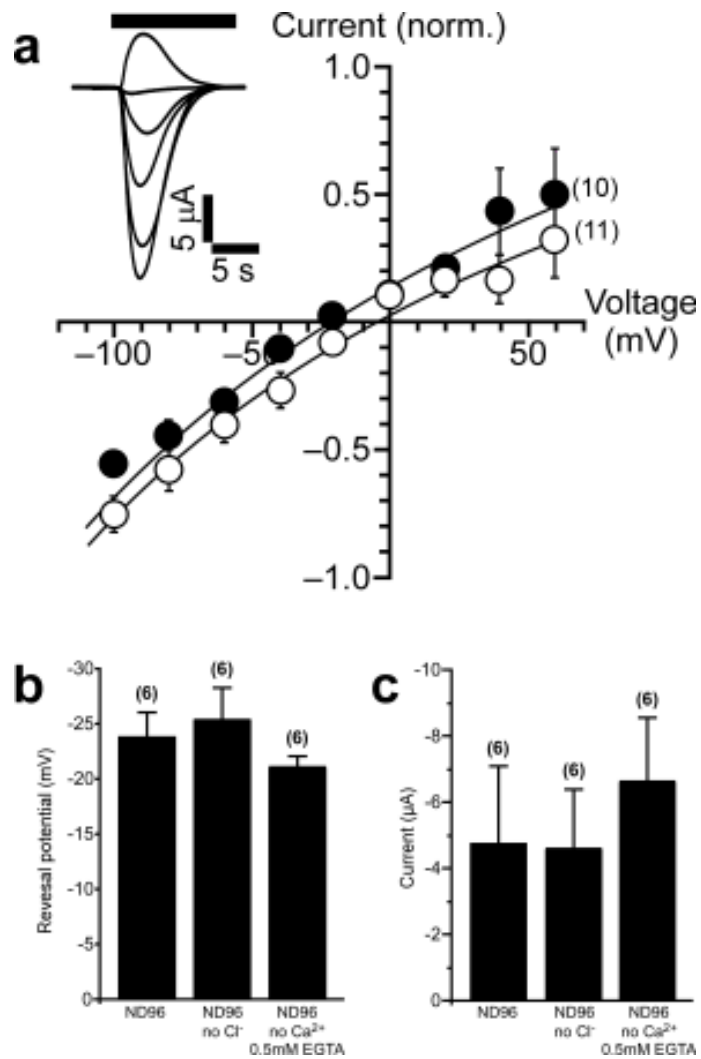
Figure 3. Ion selectivity of AvGluR1. (**a**) Current-voltage relationship of AvGluR1 in Na$^+$ (solid circles) and K$^+$ (open circles) extracellular solution. The reversal potential shifts by 19.7 mV from -24.3 to -2.5 mV. Inset: Representative Glu gated currents at -100, -80, -60, -40, -20 to 0 mV in Na$^+$ extracellular solution. (**b, c**) Reversal potentials (**b**) and current amplitudes (**c**) in normal extracellular ND96 solution (containing 1.8 mM Ca^{2+}), Ca^{2+}-free ND96 (zero added extracellular Ca^{2+} with 0.5 mM EGTA) and Cl$^-$-free ND96 (Cl$^-$ is replaced with gluconate). In (**b**) and (**c**) number of observations shown in parentheses and ns indicates no statistically significant differences using the Student's *t*-test (P ≥ 0.4).
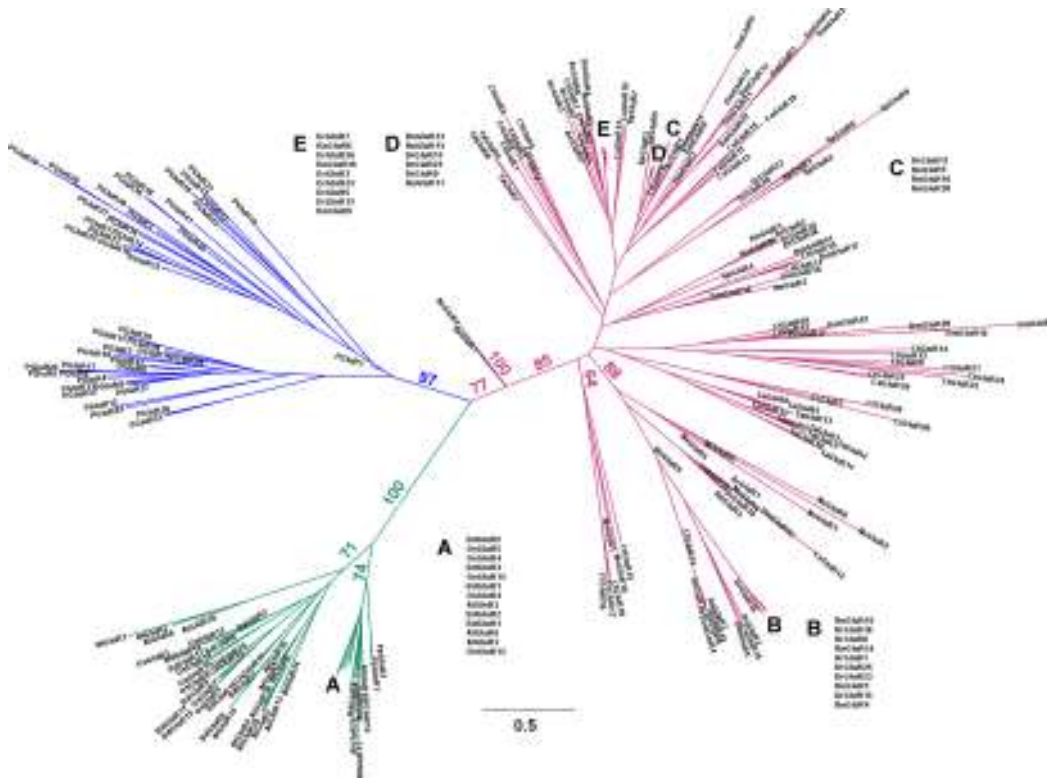
Figure 4. Maximum likelihood (ML) tree of AvGluR1 and iGluRs. 251 iGluR sequences were collected from all three kingdoms of life and the ML tree was constructed as described in the Methods. Bootstrap support values are shown at the major branches. Taxa and branches are color coded with bacteria in blue, plants in green, animals in magenta and AvGluR1 and AvGluR2 in purple.

References

1. Traynelis, S.F*., et al.* Glutamate receptor ion channels: structure, regulation, and function. *Pharmacol. Rev.* **62**, 405-496 (2010).
2. Hille, B. Chapter 22: Evolution and Origins. in *Ion channels of excitable membranes* (Sinauer Associates, Inc., Sunderland, MA, 2001).
3. Tikhonov, D.B. & Magazanik, L.G. Origin and molecular evolution of ionotropic glutamate receptors. *Neurosci. Behav. Physiol.* **39**, 763-773 (2009).
4. Kuner, T., Seeburg, P.H. & Guy, H.R. A common architecture for K+ channels and ionotropic glutamate receptors? *Trends Neurosci.* **26**, 27-32 (2003).
5. Chen, G.Q., Cui, C., Mayer, M.L. & Gouaux, E. Functional characterization of a potassium-selective prokaryotic glutamate receptor. *Nature* **402**, 817-821 (1999).
6. Wo, Z.G. & Oswald, R.E. Unraveling the modular design of glutamate-gated ion channels. *Trends Neurosci.* **18**, 161-168 (1995).
7. Wood, M.W., VanDongen, H.M. & VanDongen, A.M. Structural conservation of ion conduction pathways in K channels and glutamate receptors. *Proc. Natl. Acad. Sci. USA* **92**, 4882-4886 (1995).
8. Lam, H.M*., et al.* Glutamate-receptor genes in plants. *Nature* **396**, 125-126 (1998).
9. Gladyshev, E.A., Meselson, M. & Arkhipova, I.R. Massive horizontal gene transfer in bdelloid rotifers. *Science* **320**, 1210-1213 (2008).
10. Kumar, J., Schuck, P., Jin, R. & Mayer, M.L. The N-terminal domain of GluR6-subtype glutamate receptor ion channels. *Nat. Struct. Mol. Biol.* **16**, 631-638 (2009).
11. Egebjerg, J., Bettler, B., Hermans-Borgmeyer, I. & Heinemann, S. Cloning of a cDNA for a glutamate receptor subunit activated by kainate but not AMPA. *Nature* **351**, 745-748 (1991).
12. Fay, A.M., Corbeil, C.R., Brown, P., Moitessier, N. & Bowie, D. Functional characterization and in silico docking of full and partial GluK2 kainate receptor agonists. *Mol. Pharmacol.* **75**, 1096-1107 (2009).
13. Patneau, D.K. & Mayer, M.L. Structure-activity relationships for amino acid transmitter candidates acting at N-methyl-D-aspartate and quisqualate receptors. *J. Neurosci.* **10**, 2385-2399 (1990).
14. Herb, A*., et al.* The KA-2 subunit of excitatory amino acid receptors shows widespread expression in brain and forms ion channels with distantly related subunits. *Neuron* **8**, 775-785 (1992).
15. Jatzke, C., Watanabe, J. & Wollmuth, L.P. Voltage and concentration dependence of Ca(2+) permeability in recombinant glutamate receptor subtypes. *J. Physiol.* **538**, 25-39 (2002).
16. Schroeder, B.C., Cheng, T., Jan, Y.N. & Jan, L.Y. Expression cloning of TMEM16A as a calcium-activated chloride channel subunit. *Cell* **134**, 1019-1029 (2008).
17. Stamatakis, A. RAxML-VI-HPC: maximum likelihood-based phylogenetic analyses with thousands of taxa and mixed models. *Bioinformatics* **22**, 2688-2690 (2006).
18. Krishnamurthy, N., Brown, D. & Sjolander, K. FlowerPower: clustering proteins into domain architecture classes for phylogenomic inference of protein function. *BMC Evol Biol* **7 Suppl 1**, S12 (2007).
19. Srivastava, M*., et al.* The Amphimedon queenslandica genome and the evolution of animal complexity. *Nature* **466**, 720-726.
20. Syvanen, M. Horizontal gene transfer: evidence and possible consequences. *Annu. Rev. Genet.* **28**, 237-261 (1994).
21. Mayer, M.L. & Armstrong, N. Structure and function of glutamate receptor ion channels. *Annu. Rev. Physiol.* **66**, 161-181 (2004).
22. Silbering, A.F. & Benton, R. Ionotropic and metabotropic mechanisms in chemoreception: 'chance or design'? *EMBO Rep.* **11**, 173-179 (2010).
23. Murata, Y., Iwasaki, H., Sasaki, M., Inaba, K. & Okamura, Y. Phosphoinositide phosphatase activity coupled to an intrinsic voltage sensor. *Nature* **435**, 1239-1243 (2005).

24. Larkin, M.A.*, et al.* Clustal W and Clustal X version 2.0. *Bioinformatics* **23**, 2947-2948 (2007).

25. Shealy, R.T., Murphy, A.D., Ramarathnam, R., Jakobsson, E. & Subramaniam, S. Sequence-function analysis of the K+-selective family of ion channels using a comprehensive alignment and the KcsA channel structure. *Biophys. J.* **84**, 2929-2942 (2003).

26. Edgar, R.C. MUSCLE: a multiple sequence alignment method with reduced time and space complexity. *BMC Bioinformatics* **5**, 113 (2004).

27. Gascuel, O. BIONJ: an improved version of the NJ algorithm based on a simple model of sequence data. *Mol. Biol. Evol.* **14**, 685-695 (1997).

28. Krishnamurthy, N., Brown, D. & Sjolander, K. FlowerPower: clustering proteins into domain architecture classes for phylogenomic inference of protein function. *BMC Evol. Biol.* **7 Suppl 1**, S12 (2007).

A modern ionotropic glutamate receptor with a K$^+$ selectivity signature sequence

H. Janovjak, G. Sandoz and E.Y. Isacoff[*]

* Correspondence should be addressed to E.Y.I. (ehud@berkeley.edu).

Supplementary Figures
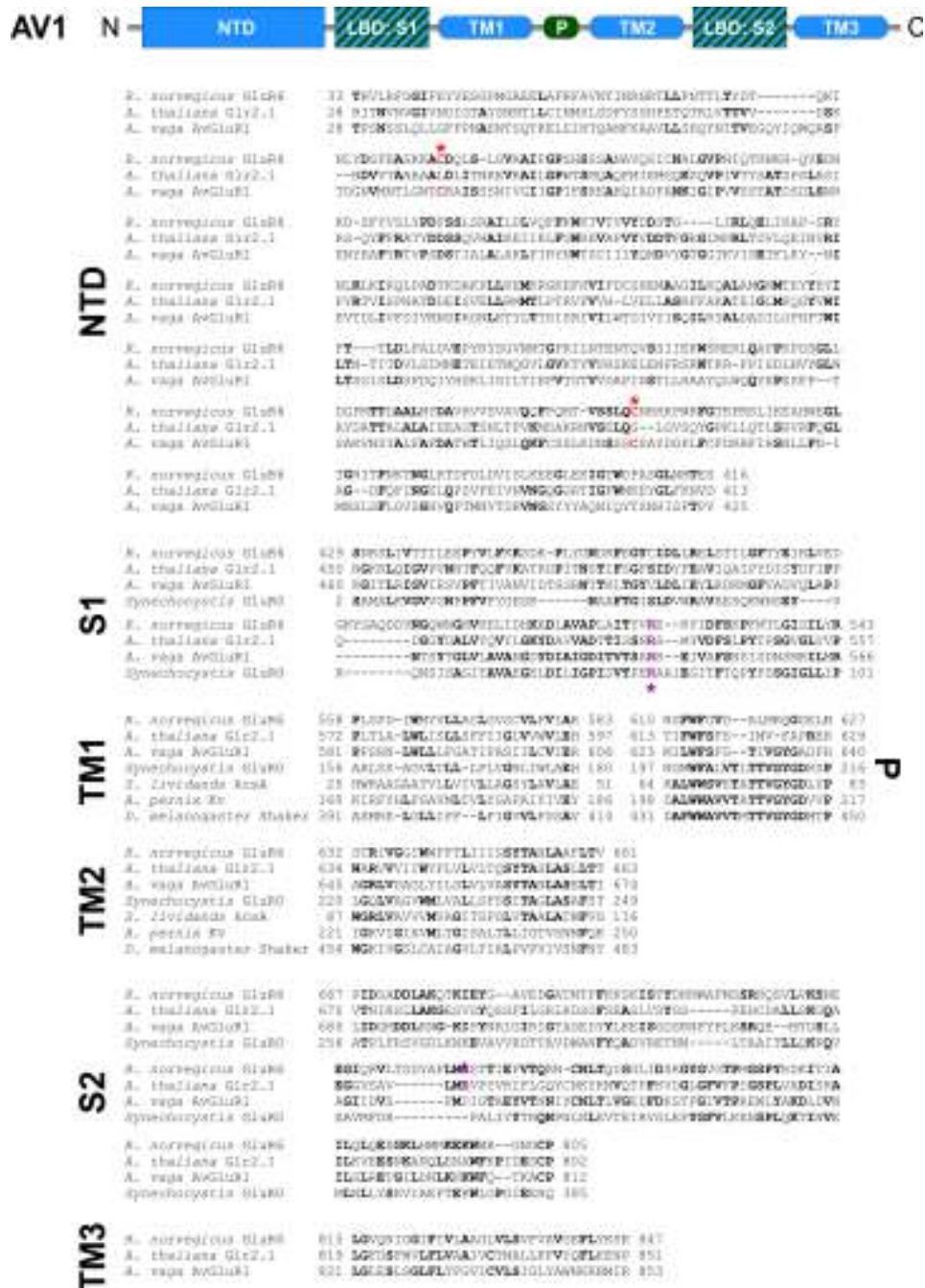
Supplementary Figure S1. Multiple sequence alignment of iGluRs and K$^+$ channels. Domains of iGluRs and K$^+$ channels were aligned using Muscle. For NTD, S1, S2 and TM3 residues in bold are found in at least two sequences. For TM1, P and TM2 residues in bold are found in at least three sequences. Key functional residues are highlighted in color (see main text for details).
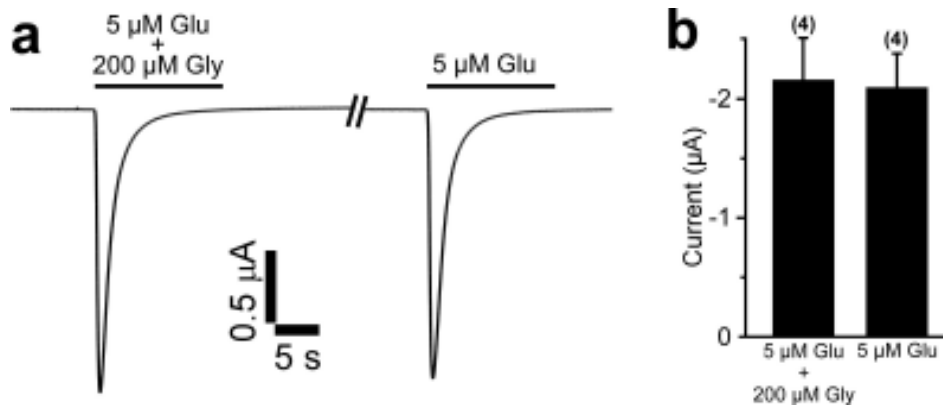
Supplementary Figure S2. No synergistic effect of glutamate gating by glycine. (**a**) Representative glutamate-gated currents near the EC50 concentration in the presence or absence of 200 µM glycine. (**b**) Current amplitudes in the presence or absence of 200 µM glycine. Means are not significantly different (P = 0.67, Student's *t*-test). Error bars are s.e.m.
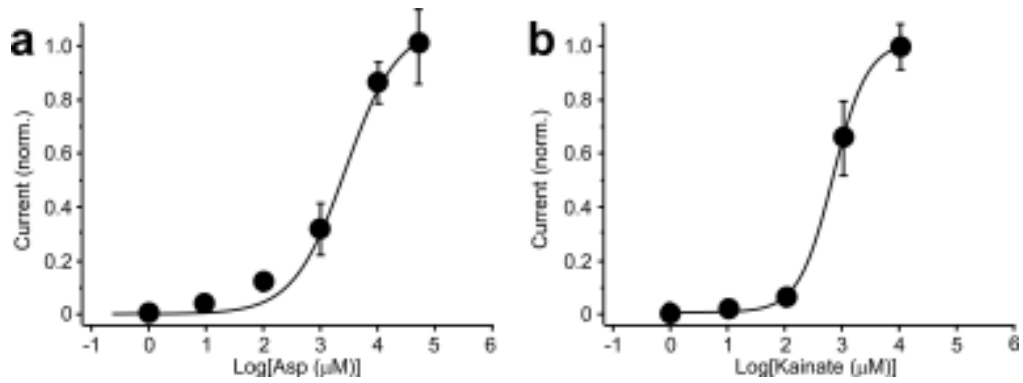
Supplementary Figure S3. Dose-response curves for aspartate and kainate. (**a**) For aspartate, we measured an EC50 of 1.8 mM (95% confidence interval 0.1 to 32.5 mM, h = 1.0, n = 6). (**b**) For kainate measured an EC50 of 0.7 mM (95% confidence interval 0.1 to 4.6 mM, h = 1.5, n = 5). At the EC50 the current amplitudes extracted from the fit were 10.4, 8.2 and 12.3 μA for glutamate, aspartate and kainate, respectively. Error bars are s.e.m.
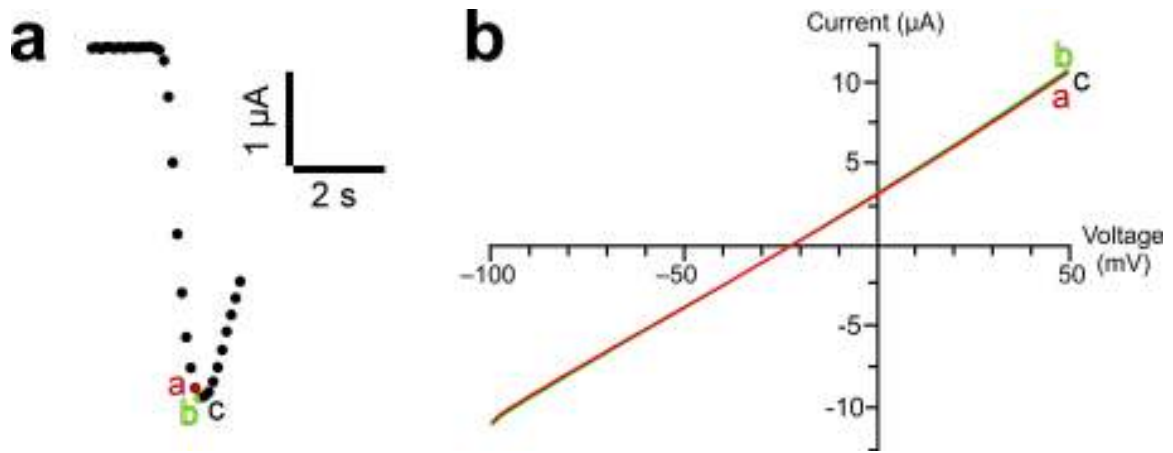
Supplementary Figure S4. Current-voltage relationships obtained at the current peak. (**a**) Current amplitude at -40 mV in response to repeated short voltage ramps. (a, b and c mark measurements evoked by three successive ramps near the peak of the current response.) (**b**) Current-voltage relationships obtained from successive ramps a, b and c, indicated in (**a**), around the current peak. Ramps were from -100 mV to 50 mV, 70 ms in duration, applied once every 100 ms. These three voltage-ramps produce nearly identical current responses and zero-crossings.

Supplementary Tables

AvGluR1 vs. Domain	GluR6	Glr2.1	GluR0	kcsA	kvAP	Shaker
NTD	9	12				
LBD	23	18	17			
TM1	**34**	**23**	19	19	15	16
P	20	31	19	**38**	**33**	14
TM2	**38**	**51**	32	27	3	16
TM3	21	20				

Supplementary Table S1. Percent sequence identity between AvGluR1 and iGluRs, GluR0 and K$^+$ channels for different domains. For TM1, P and TM2 numbers in bold indicate the highest scores. Identities were determined manually after alignment.

Species name	Abbreviation in tree	Number of proteins collected	Source
ANIMALS			
Adineta vaga	Av	2	NCBI
Aplysia californica	Ac	12	NCBI
Caenorhabditis elegans	Ce	10	NCBI
Capitella teleta	Ct	26	Joint Genome Institute (JGI)
Drosophila melanogaster	Dm	22	NCBI
Danio rerio	Dr	28	NCBI
Nematostella vectensis	Nv	10	NCBI
Rattus norvegicus	Rn	18	NCBI
Strongylocentrotus purpuratus	Sp	8	NCBI
Trichoplax adherens	Ta	13	NCBI
PLANTS			
Arabidopsis thaliana	At	20	NCBI
Brachypodium distachyon	Bd	16	JGI
Oryza sativa japonica	Os	19	NCBI
Physcomitrella patens	Pp	2	NCBI
BACTERIA	P	45	NCBI

Supplementary Table S2. Organisms searched for iGluRs and number of sequences identified.

Name in tree	Accession number	Label
ANIMALS		
Adineta vaga		
AvGluR1	ACD54595	AvGluR1
AvGluR2	ACD54612	AvGluR2
Aplysia californica		
AcGluR1	AAO46102.1	NMDA-like receptor splice form
AcGluR3	AAP41203.1	Glutamate receptor subunit protein GluR1
AcGluR2	ACA13599.1	NR2
AcGluR4	AAP41204.1	Glutamate receptor subunit protein GluR2
AcGluR5	AAP41205.1	Glutamate receptor subunit protein GluR3
AcGluR6	AAP41206.1	Glutamate receptor subunit protein GluR4
AcGluR7	AAP41207.1	Glutamate receptor subunit protein GluR5
AcGluR8	AAP41208.1	Glutamate receptor subunit protein GluR6
AcGluR9	AAP41209.1	Glutamate receptor subunit protein GluR7
AcGluR10	ACB05517.1	Glutamate receptor 8
AcGluR11	ACB05519.1	Glutamate receptor 10
AcGluR12	ACV91076.1	Glutamate receptor subunit protein GluR10
Caenorhabditis elegans		
CeGluR1	NP_492017.3	Glutamate receptor family (AMPA) family member (glr-3)
CeGluR2	NP_495033.2	NMDA class glutamate receptor family member (nmr-1)
CeGluR3	NP_495639.2	Glutamate receptor family (AMPA) family member (glr-4)
CeGluR4	NP_498887.2	Glutamate receptor family (AMPA) family member (glr-1)
CeGluR5	NP_505244.1	Glutamate receptor family (AMPA) family member (glr-5)
CeGluR6	NP_506694.3	NMDA class glutamate receptor family member (nmr-2)
CeGluR7	NP_508441.3	Glutamate receptor family (AMPA) family member (glr-7)
CeGluR8	NP_509097.1	Glutamate receptor family (AMPA) family member (glr-8)
CeGluR9	NP_741822.2	Glutamate receptor family (AMPA) family member (glr-6)
CeGluR10	NP_001021114.1	Glutamate receptor family (AMPA) family member (glr-2)
Capitella teleta		
CtGluR1	Capca1_167269	estExt_Genewise1Plus.C_7930005
CtGluR2	Capca1_225637	estExt_fgenesh1_pg.C_6130009
CtGluR3	Capca1_96910	e_gw1.129.67.1
CtGluR4	Capca1_169825	estExt_Genewise1Plus.C_400002
CtGluR5	Capca1_148073	estExt_Genewise1.C_2340020
CtGluR6	Capca1_178222	estExt_Genewise1Plus.C_6130023
CtGluR7	Capca1_164454	estExt_Genewise1.C_110088
CtGluR8	Capca1_165192	estExt_Genewise1.C_1720029
CtGluR9	Capca1_92293	e_gw1.793.5.1
CtGluR10	Capca1_179176	estExt_Genewise1Plus.C_1620047
CtGluR11	Capca1_24092	gw1.784.1.1
CtGluR12	Capca1_211454	fgenesh1_pg.C_scaffold_463000011
CtGluR13	Capca1_222580	estExt_fgenesh1_pg.C_1460013
CtGluR14	Capca1_194620	fgenesh1_pg.C_scaffold_1131000005
CtGluR15	Capca1_92735	e_gw1.190.20.1
CtGluR16	Capca1_124092	e_gw1.50.47.1

CtGluR17	Capca1_43271	gw1.20.62.1
CtGluR18	Capca1_103666	e_gw1.20.60.1
CtGluR19	Capca1_152072	estExt_Genewise1.C_8280002
CtGluR20	Capca1_218867	estExt_fgenesh1_pg.C_9520005
CtGluR21	Capca1_107912	e_gw1.1488.1.1
CtGluR22	Capca1_188571	fgenesh1_pg.C_scaffold_271000033
CtGluR23	Capca1_185470	fgenesh1_pg.C_scaffold_119000020
CtGluR24	Capca1_204960	fgenesh1_pg.C_scaffold_452000007
CtGluR25	Capca1_189895	fgenesh1_pg.C_scaffold_517000010
CtGluR26	Capca1_164990	estExt_Genewise1.C_3140016
Drosophila melanogaster		
DmGluR1	AAA28574.1	Glutamate receptor subunit
DmGluR2	AAA28575.1	Glutamate receptor subunit kainate subtype
DmGluR3	AAC00192.1	Glutamate receptor DGluRIIB
DmGluR4	AAL39343.1	GH25591p
DmGluR5	AAM46167.1	AF381249_1 NMDA receptor 2
DmGluR6	AAM49854.1	HL08030p
DmGluR7	AAM50963.1	RE06730p
DmGluR8	NP_730940.1	NMDA receptor 1
DmGluR9	AAN71127.1	AT31673p
DmGluR10	NP_727328.1	Ionotropic receptor 8a
DmGluR11	AAV36909.1	RE13419p
DmGluR12	AAV36912.1	RE07945p
DmGluR13	AAX51647.1	RE24732p
DmGluR14	NP_649176.1	Ionotropic receptor 76b
DmGluR15	NP_572795.1	Ionotropic receptor 11a
DmGluR16	NP_572411.1	Ionotropic receptor 7c
DmGluR17	ACU43550.1	IP13516p
DmGluR18	NP_001137969.1	Ionotropic receptor 75d
DmGluR19	NP_001137966.2	Ir75b
DmGluR20	NP_001097043.1	Ionotropic receptor 21a
DmGluR21	NP_001036735.1	CG5621
DmGluR22	NP_001036373.1	clumsy
Danio rerio		
DrGluR1	XP_699070.4	PREDICTED: Glutamate receptor
DrGluR2	AAI62459.1	Glutamate receptor
DrGluR3	AAI62505.1	Glutamate receptor
DrGluR4	XP_693260.4	PREDICTED: Glutamate-like
DrGluR5	AAI62620.1	Glutamate receptor
DrGluR6	XP_694772.3	PREDICTED: Glutamate-like
DrGluR7	AAL13229.1	AF361751_1 AMPA receptor subunit 2b
DrGluR8	XP_691754.2	PREDICTED: similar to N-methyl-D-aspartate receptor channel subunit epsilon 1
DrGluR9	XP_690040.3	PREDICTED: Glutamate receptor 5-like
DrGluR10	XP_685683.3	PREDICTED: Glutamate receptor delta-1 subunit-like
DrGluR11	XP_684512.3	PREDICTED: Glutamate receptor
DrGluR12	CAM14407.1	Glutamate receptor
DrGluR13	XP_683795.4	PREDICTED: Glutamate receptor
DrGluR14	XP_002664030.1	PREDICTED: NMDA receptor NR2C subunit-like
DrGluR15	XP_002663775.1	PREDICTED: Glutamate-like
DrGluR16	XP_002661175.1	PREDICTED: NMDA receptor NR2C subunit-like
DrGluR17	NP_001074079.1	Vomeronasal 2

DrGluR18	NP_001121809.1	Glutamate [NMDA] receptor subunit epsilon-2
DrGluR19	NP_001137603.1	Glutamate receptor
DrGluR20	NP_001138274.1	si:ch211-251b21.1
DrGluR21	XP_001924038.2	PREDICTED: Glutamate receptor
DrGluR22	XP_001923977.1	PREDICTED: Kainate receptor beta subunit-like
DrGluR23	XP_001921725.1	PREDICTED: Glutamate-like
DrGluR24	NP_938174.1	Glutamate receptor
DrGluR25	XP_001921158.1	PREDICTED: N-methyl-D-aspartate receptor subunit 2D
DrGluR26	NP_991293.1	Glutamate receptor
DrGluR27	XP_001339222.3	PREDICTED: Glutamate receptor
DrGluR28	XP_001333587.2	PREDICTED: Glutamate receptor delta-1 subunit-like
Nematostella vectensis		
NvGluR1	XP_001622303.1	Hypothetical protein NEMVEDRAFT_v1g141731
NvGluR2	XP_001641049.1	Predicted protein
NvGluR3	XP_001626463.1	Predicted protein
NvGluR4	XP_001627645.1	Predicted protein
NvGluR5	XP_001629139.1	Predicted protein
NvGluR6	XP_001629614.1	Predicted protein
NvGluR7	XP_001633354.1	Predicted protein
NvGluR8	XP_001639888.1	Predicted protein
NvGluR9	XP_001636905.1	Predicted protein
NvGluR10	XP_001638696.1	Predicted protein
Rattus norvegicus		
RnGluR1	C45219	N-methyl-D-aspartate receptor chain NMDAR2D-1
RnGluR2	CAA46335.1	NMDA receptor subunit
RnGluR3	CAA78937.1	Glutamate receptor subtype delta-2
RnGluR4	NP_036707.3	Glutamate [NMDA] receptor subunit epsilon-3
RnGluR5	NP_113696.1	Glutamate receptor
RnGluR6	NP_113796.1	Glutamate receptor 1 precursor
RnGluR7	NP_579842.2	Glutamate [NMDA] receptor subunit 3B precursor
RnGluR8	P19491.2	Glutamate receptor 2
RnGluR9	P19492.1	Glutamate receptor 3
RnGluR10	P19493.1	Glutamate receptor 4
RnGluR11	P22756.3	GRIK1 Glutamate receptor
RnGluR12	P42260.2	GRIK2 Glutamate receptor
RnGluR13	P42264.1	GRIK3 Glutamate receptor
RnGluR14	Q00959.2	Glutamate [NMDA] receptor subunit epsilon-1
RnGluR15	Q00960.1	Glutamate [NMDA] receptor subunit epsilon-2
RnGluR16	Q01812.1	GRIK4 Glutamate receptor
RnGluR17	S28857	Glutamate receptor delta-1 chain precursor
RnGluR18	XP_002726571.1	PREDICTED: Glutamate receptor
Strongylocentrotus purpuratus		
SpGluR1	XP_001188377.1	PREDICTED: Similar to AMPA receptor subunit GluR3B
SpGluR2	XP_001197583.1	PREDICTED: Similar to AMPA receptor GluR3/C
SpGluR3	XP_784968.2	PREDICTED: Similar to Glutamate receptor
SpGluR4	XP_787239.2	PREDICTED: Similar to AMPA receptor GluR1/A
SpGluR5	XP_789521.2	PREDICTED: Hypothetical protein
SpGluR6	XP_792639.1	PREDICTED: Similar to glutamate receptor AMPA/kainate type
SpGluR7	XP_794826.2	PREDICTED: Similar to AMPA GluR2
SpGluR8	XP_796568.2	PREDICTED: Similar to AMPA receptor GluR2/B

Trichoplax adherens		
TaGluR1	XP_002107780.1	Hypothetical protein TRIADDRAFT_19383
TaGluR2	XP_002108129.1	Hypothetical protein TRIADDRAFT_18823
TaGluR3	XP_002108130.1	Hypothetical protein TRIADDRAFT_18262
TaGluR4	XP_002108131.1	Hypothetical protein TRIADDRAFT_18943
TaGluR5	XP_002117385.1	Hypothetical protein TRIADDRAFT_3218
TaGluR6	XP_002111317.1	Hypothetical protein TRIADDRAFT_55165
TaGluR7	XP_002112358.1	Hypothetical protein TRIADDRAFT_14565
TaGluR8	XP_002112769.1	Hypothetical protein TRIADDRAFT_25025
TaGluR9	XP_002112772.1	Hypothetical protein TRIADDRAFT_25027
TaGluR10	XP_002116223.1	Hypothetical protein TRIADDRAFT_30609
TaGluR11	XP_002116224.1	Hypothetical protein TRIADDRAFT_30612
TaGluR12	XP_002117382.1	Hypothetical protein TRIADDRAFT_32461
TaGluR13	XP_002117383.1	Hypothetical protein TRIADDRAFT_61396
PLANTS		
Arabidopsis thaliana		
AtGluR1	A84550	Probable ligand-gated ion channel protein
AtGluR2	AAB61068.1	Similar to the ligand-gated ionic channels family
AtGluR3	AAB71458.1	Similar to Arabidopsis putative ion-channel
AtGluR4	NP_199652.1	ATGLR1.3 Intracellular ligand-gated ion channel
AtGluR5	AAC33237.1	Putative ligand-gated ion channel protein
AtGluR6	AAC33239.1	Putative ligand-gated ion channel protein
AtGluR7	AAD09173.1	Putative glutamate receptor
AtGluR8	NP_199651.1	ATGLR1.2 Intracellular ligand-gated ion channel
AtGluR9	AAD50976.1	Ionotropic glutamate receptor ortholog GLR6 AF170494_1
AtGluR10	AAF02156.1	Unknown protein AC009853_16
AtGluR11	AAF21042.1	Glr5 AF210701_1
AtGluR12	AAK13248.1	Putative glutamate receptor like-protein AF159498_1
AtGluR13	NP_196682.1	ATGLR2.5 Intracellular ligand-gated ion channel
AtGluR14	NP_196679.1	ATGLR2.6 Intracellular ligand-gated ion channel
AtGluR15	NP_194899.1	ATGLR2.4 Intracellular ligand-gated ion channel
AtGluR16	NP_180474.1	ATGLR2.9 Intracellular ligand-gated ion channel
AtGluR17	AAR27949.1	GLR3.3
AtGluR18	NP_180048.1	ATGLR2.2 Intracellular ligand-gated ion channel
AtGluR19	NP_180047.1	ATGLR2.3 Intracellular ligand-gated ion channel
AtGluR20	CAB63012.1	Putative glutamate receptor
Brachypodium distachyon		
BdGluR1	Bradi1g26030	
BdGluR2	Bradi3g01620	
BdGluR3	Bradi1g32800	
BdGluR4	Bradi5g19560	
BdGluR5	Bradi1g59600	
BdGluR6	Bradi2g41790	
BdGluR7	Bradi4g30850	
BdGluR8	Bradi4g30860	
BdGluR9	Bradi1g31350	
BdGluR10	Bradi4g30880	
BdGluR11	Bradi4g30820	
BdGluR12	Bradi4g30840	

BdGluR13	Bradi4g30810	
BdGluR14	Bradi3g53690	
BdGluR15	Bradi1g46910	
BdGluR16	Bradi3g51890	
Oryza sativa japonica		
OsGluR1		116309819_emb_CAH668
OsGluR2	EAY87800.1	Hypothetical protein OsI_09220
OsGluR3	EAY99961.1	Hypothetical protein OsI_21965
OsGluR4	EAZ02098.1	Hypothetical protein OsI_24185
OsGluR5	EAZ02474.1	Hypothetical protein OsI_24580
OsGluR6	EEC80160.1	Hypothetical protein OsI_21975
OsGluR7	EAZ09182.1	Hypothetical protein OsI_31453
OsGluR8	EAZ09183.1	Hypothetical protein OsI_31454
OsGluR9	EAZ09184.1	Hypothetical protein OsI_31456
OsGluR10	EAZ09187.1	Hypothetical protein OsI_31459
OsGluR11	EAZ09194.1	Hypothetical protein OsI_31466
OsGluR12	EEC72350.1	Hypothetical protein OsI_05591
OsGluR13	EEC80154.1	Hypothetical protein OsI_21964
OsGluR14	EEC82165.1	Hypothetical protein OsI_26240
OsGluR15	EEC80159.1	Hypothetical protein OsI_21973
OsGluR18	EEC84618.1	Hypothetical protein OsI_31464
OsGluR19	EEC84617.1	Hypothetical protein OsI_31458
Physcomitrella patens		
PpGluR1	XP_001762626.1	Predicted protein
PpGluR2	XP_001779207.1	Predicted protein
BACTERIA		
PGluR1	ZP_05036786.1	Bacterial extracellular solute-binding protein family 3 [Synechococcus sp. PCC 7335]
PGluR2	ZP_05043015.1	Bacterial extracellular solute-binding protein family 3 [Alcanivorax sp. DG881]
PGluR3	NP_441171.1	Hypothetical protein slr1257 [Synechocystis sp. PCC 6803]
PGluR4	NP_894348.1	GIC family ligand gated channel [Prochlorococcus marinus str. MIT 9313]
PGluR5	NP_896860.1	GIC family ligand gated channel [Synechococcus sp. WH 8102]
PGluR6	ZP_05044674.1	Ionotropic glutamate receptor [Cyanobium sp. PCC 7001]
PGluR7	YP_001130102.1	Extracellular solute-binding protein [Prosthecochloris vibrioformis DSM 265]
PGluR8	YP_001224896.1	Hypothetical protein SynWH7803_1173 [Synechococcus sp. WH 7803]
PGluR9	YP_001227767.1	Hypothetical protein SynRCC307_1511 [Synechococcus sp. RCC307]
PGluR10	YP_001733604.1	Periplasmic substrate binding protein [Synechococcus sp. PCC 7002]
PGluR11	YP_001803825.1	Extracellular solute-binding protein [Cyanothece sp. ATCC 51142]
PGluR12	YP_001805997.1	Ligand gated channel [Cyanothece sp. ATCC 51142]
PGluR13	YP_001869676.1	Extracellular solute-binding protein [Nostoc punctiforme PCC 73102]
PGluR14	YP_001960498.1	Ion transport 2 domain protein [Chlorobium phaeobacteroides BS1]
PGluR15	YP_001997058.1	Extracellular solute-binding protein family 3 [Chloroherpeton thalassium ATCC 35110]
PGluR16	YP_001997839.1	Extracellular solute-binding protein family 3 [Chlorobaculum parvum NCIB 8327]
PGluR17	ZP_05788417.1	Ionotropic glutamate receptor [Synechococcus sp. WH 8109]
PGluR18	YP_002954183.1	Bacterial extracellular solute-binding protein [Desulfovibrio magneticus RS-1]
PGluR19	YP_003267580.1	Extracellular solute-binding protein family 3 [Haliangium ochraceum DSM 14365]
PGluR20	YP_003585093.1	Ligand-gated ion channel family protein [Zunongwangia profunda SM-A87]
PGluR21	YP_321508.1	Ionotropic glutamate receptor [Anabaena variabilis ATCC 29413]

PGluR22	YP_339120.1	Extracellular solute-binding protein [Pseudoalteromonas haloplanktis TAC125]
PGluR23	YP_374461.1	Extracellular solute-binding protein [Chlorobium luteolum DSM 273]
PGluR24	YP_376778.1	Ionotropic glutamate receptor [Synechococcus sp. CC9902]
PGluR25	YP_378562.1	Extracellular solute-binding protein [Chlorobium chlorochromatii CaD3]
PGluR26	YP_723930.1	Extracellular solute-binding protein [Trichodesmium erythraeum IMS101]
PGluR27	YP_730938.1	GIC family ligand gated channel [Synechococcus sp. CC9311]
PGluR28	YP_861587.1	Ligand-gated ion channel family protein [Gramella forsetii KT0803]
PGluR29	ZP_00517290.1	Extracellular solute-binding protein family 3:Bacterial extracellular solute-binding protein family 3 [Crocosphaera watsonii WH 8501]
PGluR30	ZP_01042624.1	Extracellular solute-binding protein family 3 [Idiomarina baltica OS145]
PGluR31	ZP_01080226.1	Possible ligand gated channel (GIC family protein) [Synechococcus sp. RS9917]
PGluR32	ZP_01085070.1	Possible ligand gated channel (GIC family protein) [Synechococcus sp. WH 5701]
PGluR33	ZP_01124154.1	Possible ligand gated channel (GIC family) protein [Synechococcus sp. WH 7805]
PGluR34	ZP_01437479.1	Extracellular solute-binding protein family 3 [Fulvimarina pelagi HTCC2506]
PGluR35	ZP_06369637.1	Extracellular solute-binding protein family 3 [Desulfovibrio sp. FW1012B]
PGluR36	ZP_01628414.1	Possible ligand gated channel (GIC family) [Nodularia spumigena CCY9414]
PGluR37	ZP_01691371.1	Extracellular solute-binding protein family 3 [Microscilla marina ATCC 23134]
PGluR38	ZP_01720436.1	Hypothetical protein ALPR1_14489 [Algoriphagus sp. PR1]
PGluR39	ZP_01731352.1	Possible ligand gated channel (GIC family) protein [Cyanothece sp. CCY0110]
PGluR40	ZP_01893479.1	Extracellular solute-binding protein family 3 [Marinobacter algicola DG893]
PGluR41	ZP_01909425.1	Extracellular solute-binding protein family 3 [Plesiocystis pacifica SIR-1]
PGluR42	ZP_02003278.1	Bacterial extracellular solute-binding protein family 3 [Beggiatoa sp. PS]
PGluR43	ZP_03130928.1	Extracellular solute-binding protein family 3 [Chthoniobacter flavus Ellin428]
PGluR44	ZP_03157700.1	Ion transport 2 domain protein [Cyanothece sp. PCC 7822]
PGluR45	ZP_05023856.1	Bacterial extracellular solute-binding protein family 3 [Microcoleus chthonoplastes PCC 7420]

Supplementary Table S3. iGluR sequences included in the phylogenetic analysis.